

Article

The Thermal State of the North Atlantic Ocean and Hydrological Droughts in the Warta River Catchment in Poland during 1951–2020

Andrzej A. Marsz ¹, Leszek Sobkowiak ^{2,*} , Anna Styszyńska ¹, Dariusz Wrześniński ²  and Adam Perz ² 

¹ Association of Polish Climatologists, Krakowskie Przedmieście Str. 30, 00-927 Warsaw, Poland; aamarsz127@gmail.com (A.A.M.); astys19@wp.pl (A.S.)

² Department of Hydrology and Water Resources Management, Faculty of Geographical and Geological Sciences, Adam Mickiewicz University, Bogumiła Krygowskiego Str. 10, 61-680 Poznań, Poland; darwrze@amu.edu.pl (D.W.); adam.perz@amu.edu.pl (A.P.)

* Correspondence: lesob@amu.edu.pl

Abstract: This study presents the direct relationships between changes in the annual surface temperature of the North Atlantic (SST) and the number of days per year experiencing low flows in the Warta River catchment (WRC) in Central Europe, Poland, in the multi-annual period of 1951–2020. The number of days experiencing low flows (T_{LF}) was used to describe the conditions of hydrological drought in the WRC. Moderately strong ($r \sim 0.5$) but statistically highly significant ($p < 0.001$) relationships were found between T_{LF} and the SST in the subtropical (30–40° N, 60–40° W) and subpolar North Atlantic (70° N, 10° W–10° E). With the increase in the annual SST in these parts of the North Atlantic, the number of days in a year experiencing low flows in the WRC also increased. It was determined that besides synchronous (i.e., in the same year) relationships between T_{LF} and SST, asynchronous relations also occurred: the SST changes were one year ahead of the T_{LF} changes. With the increase in the SST in the subtropical and subpolar North Atlantic, the sunshine duration and air temperature in the WRC increased, while the relative humidity decreased. The relationships between precipitation in the WRC and SST were negative (from -0.04 to -0.14), but statistically insignificant ($p > 0.2$). This indicates that the impact of SST changes on T_{LF} in the WRC is mainly caused by the shaping of the amount of surface evaporation, which strongly increases in years of high SST, and the climatic water balance becomes negative, resulting in an increase in extremely low flows. The analysis of the causes of these relationships shows that the SST changes in the North Atlantic control, through changes in the height of the geopotential (h_{500}), changes in the atmospheric circulation over Europe. In the periods of SST h_{500} growth over Central Europe, the atmospheric pressure (SLP) increases. That area is more frequently than average under the influence of the Azores High; this leads to an increase in the frequency of anticyclonic weather. A significant increase in the number of T_{LF} s and prolonged periods of hydrological drought in the WRC after 2000 are associated with a strong increase in the SST in the area of the tropical and subtropical North Atlantic.

Keywords: North Atlantic sea surface temperature; Warta River catchment; droughts; river low flows; teleconnections



Citation: Marsz, A.A.; Sobkowiak, L.; Styszyńska, A.; Wrześniński, D.; Perz, A. The Thermal State of the North Atlantic Ocean and Hydrological Droughts in the Warta River Catchment in Poland during 1951–2020. *Water* **2023**, *15*, 2547. <https://doi.org/10.3390/w15142547>

Academic Editor: Maria Mimikou

Received: 25 June 2023

Revised: 9 July 2023

Accepted: 10 July 2023

Published: 12 July 2023



Copyright: © 2023 by the authors. Licensee MDPI, Basel, Switzerland. This article is an open access article distributed under the terms and conditions of the Creative Commons Attribution (CC BY) license (<https://creativecommons.org/licenses/by/4.0/>).

1. Introduction

In Poland, as in almost all of Europe, the frequency of droughts is increasing. A clear increase in the frequency of droughts and their intensity is also recorded in Central Europe, where droughts occurring in the 21st century have turned out to have no analogues in the past several hundred years [1]. The drought that affected Central Europe in 2015 was extremely severe [2], and according to [3], the droughts in 2018–2019 in Germany were the most extreme since the beginning of the 16th century. Data from Poland fully confirm this picture; the frequency and intensity of droughts has been increasing since the turn of

the 20th and 21st centuries [4], leading to an almost continuous drought period of great severity in the last decade.

Droughts are a multi-faceted phenomenon, characterized by a varied duration, intensity and spatial distribution [5]. The prolonged dry-weather period leads to a decrease in surface runoff, and usually, combined with a high temperature and low air humidity, results in a gradual decrease in water resources in the soil. Drought goes from the stage of meteorological drought to the stage of soil drought, in which, along with its increasing duration, it is transformed into agricultural drought. The depletion of water resources in the ground, including the first groundwater level, reduces the underground supply of surface waters, especially rivers. River flow decreases and at some point the drought goes to the stage of hydrological drought.

Meteorological and soil droughts are distinguished on the basis of different criteria, and various indicators are used for this purpose [6]. The onset of agricultural drought depends not only on the course of meteorological processes, but also on the mechanical composition of the soil, water resources retained in previous periods, and the water demand of plant species growing on a given area [7]. In the case of agricultural drought, in view of the different responses of individual crop species to water shortages in the soil and the diversity of the mechanical composition of soils and relief, it is difficult to determine the exact moment of its beginning and the extent of the area in which the drought occurs. In some cases, there may already be clear signs of drought in some agricultural areas, even though the Palmer drought index or other indices used do not yet indicate drought. In other cases, while the indices based on meteorological data may validate the occurrence of drought, the assessment of the condition of crops does not confirm it.

Agricultural drought, especially when it lasts for a long time or/and is characterized by a high intensity, leads to such significant disturbances in the water balance that it transforms into a hydrological drought. The occurrence of hydrological drought is manifested most obviously in a decrease in river flows below the average value for a given period and the occurrence of low flows [8,9], i.e., a period with an uninterrupted sequence of daily flows lower than the arbitrarily adopted threshold value. Despite the fact that the low flow is also a multi-dimensional and thus complex process [10], it is possible to establish criteria at a given water gauge that enable one to unambiguously determine its beginning and end. This enables one to characterize the hydrological drought occurring in different areas (catchments) in a comparable manner, defining its duration. In the analysis of the occurrence of hydrological drought in a given catchment (low water in a given river), not only changes in the course of climatic elements, but also all other characteristics of the environment of a given catchment that affect the water cycle within its boundaries (catchment geology, groundwater resources, land use, etc.) are taken into account. Hydrological drought is an extreme phenomenon and its occurrence leads not only to great losses in crops, but also to significant losses in forest management, and serious problems in municipal water management and the power industry.

The occurrence of droughts is caused by specific weather conditions over a given area—cloudless or low-cloud weather for a long time, a lack of precipitation, high solar radiation, high air temperature and low relative humidity. Such weather conditions in the warm season contribute, through a very strong increase in evaporation, to deepening the water deficit.

Weather conditions depend on the synoptic conditions over a given area, and these, as synoptic meteorology shows, are conditioned by the course of large-scale atmospheric circulation. Since changes in atmospheric circulation around the North Atlantic (NA), including over Europe, are controlled by changes in the thermal state of the NA (e.g., [11–22]), droughts show a direct relationship with the thermal state of the NA (e.g., [23–26]).

The long-term variability in river flows and the occurrence of droughts in Poland are related to the phases of the thermohaline circulation in the NA (hereinafter referred to as NA THC) [27–29]. This indicates that changes in the thermal state of the NA affect changes in the elements of the water balance in this area. Since the NA THC variability is one of

the factors controlling the variation in the North Atlantic sea surface temperature (NA SST) (e.g., [11,13,30,31]), it can be assumed that the occurrence of hydrological droughts in Poland should show a different strength of relationship with the variability in the SST of individual parts of the NA.

The question arises as to what the relationships between the SST variability in the North Atlantic, its spatial distribution, and the occurrence of hydrological droughts are. The Warta River catchment (WRC), the third longest river in Poland, was selected as the study area. It is located in the western part of Poland, and it covers about 54.5 thousand km², which is larger than some European countries (e.g., Denmark, Belgium or the Netherlands). The climatic conditions in the WRC, i.e., a relatively high annual air temperature and a low and significant annual variability in precipitation, make that area particularly prone to frequent droughts [5,32,33]. It is especially important for the economy of that region, which is characterized by intensive and highly profitable agriculture.

The aim of this study is to present the results of studies on the relationships between the variability in the spatial distribution of the NA SST and the occurrence of hydrological droughts in the Warta River catchment (hereinafter referred to as the WRC). Several aspects were addressed in the research. The main issue was to determine those parts of the Atlantic in which the SST changes show the strongest relationship with the occurrence of hydrological droughts. An equally important question was with regard to which aspects of the meteorological regime influencing the formation of hydrological droughts in the WRC are regulated by the NA SST variability. This will allow one to answer the following question: what factors influence the variability in the surface temperature of individual parts of the ocean and impact the formation of these droughts. Attention was also paid to the mechanisms involved in the relationship between NA SST variability and the formation of hydrological droughts, i.e., extremely severe droughts. Due to the complex nature of these mechanisms, they were only briefly presented in this paper.

2. Materials and Methods

2.1. Study Area

The Warta River is the third longest river in Poland: its total length is 808 km. It is the largest right-bank tributary of the Oder (Odra) River, and most of its catchment area (54,519 km²) lies below 200 m a.s.l. [34]. However, it has a relatively diversified terrain and extends from highlands in the south through the lowlands of Central Poland to the lake district area in the north.

According to the Köppen–Geiger classification of climates, the WRC lies within the transition zone between a humid continental (Cfb) and oceanic climate (Dfb), with relatively cold winters and warm summers [35]. Woś (2010) [36] described its climate as warm, with both marine and continental characteristics, shaped primarily by the polar air masses formed over the Northern Atlantic Ocean. The average annual air temperature in the study area is about 7.5–8.5 °C, and the average annual precipitation varies from 520 mm in the north-eastern part of the catchment, to 675 mm in the southern uplands [36].

The specific runoff in the WRC shows considerable spatial differences, with the highest values in the southern (uplands) and northern areas (lake district), and the lowest in the central part. In the upper Noteć River, the average specific runoff is below 2 dm³·s⁻¹·km² (less than 70 mm), which means that that area has the lowest specific runoff in the whole of Europe, recorded only in the Caspian Lowland. According to [37], for the period of 1921–1970, the specific mean runoff was 4 dm³·s⁻¹·km², which equaled 127 mm, and the runoff coefficient was 23.9%. The annual runoff in the WRC is also spatially diversified—the highest values, exceeding 200 mm, and locally even 300 mm, are recorded in its northern and southern parts. Noticeably lower runoffs (below 150 mm, locally even below 80 mm) are in the central and western parts [38]. The average annual runoff for the WRC at the Gorzów Wielkopolski gauge is only 127 mm, which makes this region one of the poorest in Europe in terms of water resources.

According to the division proposed by [39], the rivers of the study area represent three sub-types of nival hydrological regime, namely weakly, moderately, and strongly developed [38]. Rotnicka [40], based on Ward's hierarchical grouping, distinguished 12 types of hydrological period for the rivers of the Odra River basin and the West Pomerania catchments in Poland. It was found that most rivers in the central part of the WRC represented the contrasting, five-period regime, with the deep low-water period in summer and autumn, and the high-water period in spring. In the rest of the WRC, the rivers represented mainly the four-period regime, with the average low-water period in summer–autumn, and the high-water period in early spring. Much less contrasting types of regimes are represented by rivers in the northern and southern parts of the WRC, including the three-period lowland type of regime with the average low-water period in summer–autumn and the low high-water period in late winter or early spring (the Drawa River), or even the one-period type of regime (the upper Gwda River).

In the annual discharges and the annual runoff of the Warta River, a strong autocorrelation with the one-year lag can be determined. The coefficients of autocorrelation and partial autocorrelation at the Poznań gauge are equal to 0.408. This means that the runoff in a given year strongly depends on the runoff in the previous year. In the multi-annual period of 1951–2020, the autocorrelation explains 20% of the variance in the annual runoff of the Warta River.

The geographical position of the study area and the location of the analyzed water gauges and meteorological stations are shown in Figure 1.

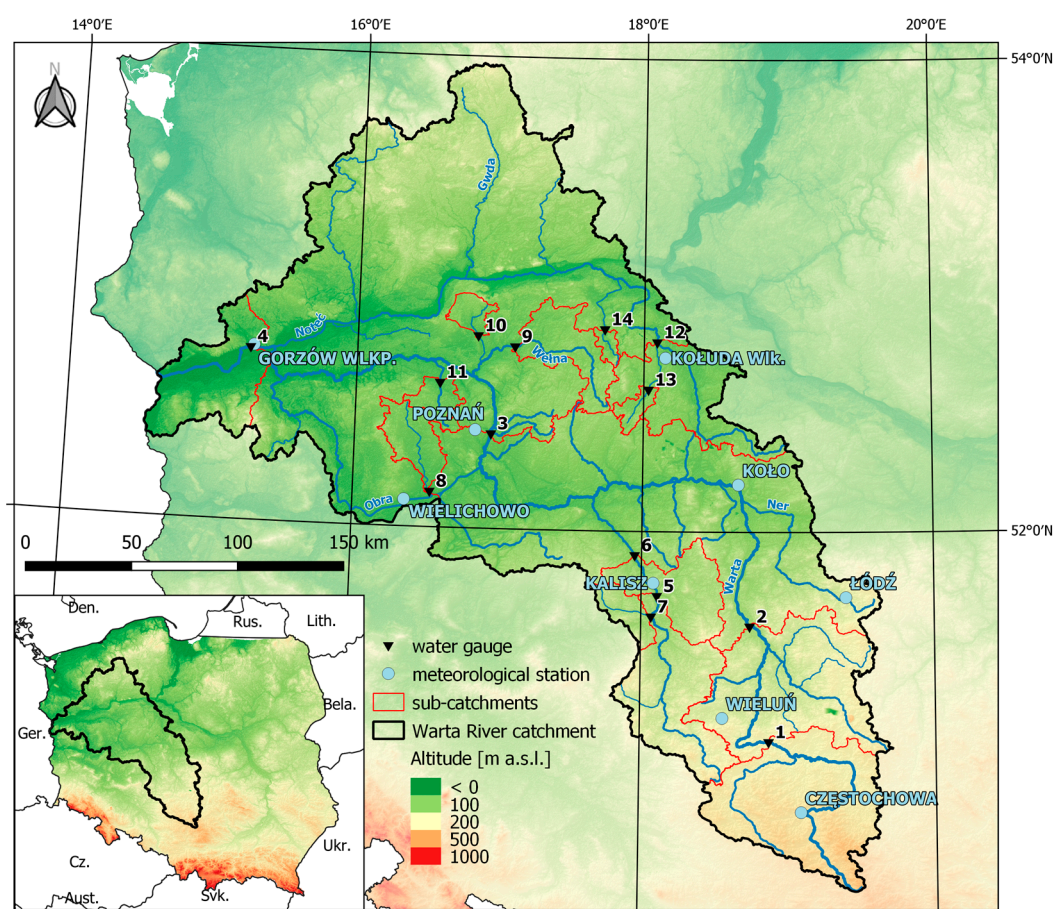


Figure 1. The geographical position of the Warta River catchment (WRC) and the location of the analyzed water gauges and meteorological stations. Note: Numbering of water gauges is accordance with Table 1.

Table 1. Major characteristics and flow regime of the analyzed rivers in the Warta River catchment (WRC) in 1951–2020.

No.	River	Gauge	Coordinates		Catchment Area [km ²]	Total Flow [mm]	Type of River Regime *
			° N	° E			
1	Warta	Działoszyn	51.1	18.9	4088	185.8	1
2	Warta	Sieradz	51.6	18.7	8140	171.3	1
3	Warta	Poznań	52.4	16.9	25,126	124.5	1
4	Warta	Gorzów Wlkp.	52.7	15.2	52,186	124.4	1
5	Prosna	Piwonice	51.7	18.1	2938	119.2	1
6	Prosna	Bogusław	51.9	18.0	4304	114.3	1
7	Ołobok	Ołobok	51.6	18.1	447	110.7	2
8	Mogilnica	Konojad	52.2	16.5	663	77.3	2
9	Wełna	Pruśce	52.8	17.1	1130	92.5	2
10	Flinta	Ryczywół	52.8	16.8	276	74.2	2
11	Sama	Szamotuły	52.6	16.6	395	83.4	2
12	Noteć	Pakość 2	52.8	18.1	1620	105.5	1
13	Noteć Zach.	Gębice	52.6	18.0	182	101.8	1
14	Gąsawka	Żnin	52.9	17.7	148	108.5	2

Note: * Types of river flow regimes: 1—nival moderately developed, 2—nival strongly developed. Source: [38], modified.

Data from 14 water gauges located on the Warta River and its tributaries (Figure 1) were used in the study. Basic data on the Warta River and its tributaries analyzed in terms of the synchronous and asynchronous occurrence of the runoff maxima are presented in Table 1.

2.2. Data

2.2.1. Meteorological and Climatic Data

The meteorological and climatic data sets for the study area were obtained from the publicly available archives of the Institute of Meteorology and Water Management—National Research Institute in Warsaw, and included monthly values of air temperature and rainfall totals, relatively evenly distributed in the WRC and its immediate vicinity. The data were recorded at the following stations: Częstochowa, Wieluń, Kalisz, Łódź, Koło, Wielichowo, Poznań, Kołuda Wielka and Gorzów (Figure 1). The annual values were calculated based on the monthly data recorded at these stations. Then, the annual average for all these stations was obtained, which enabled the area average annual temperature and annual precipitation totals for the WRC to be calculated. Additionally, data from a number of stations of various levels, including the number of days with precipitation exceeding 1 mm, relative humidity, general cloudiness, etc., were used. While all these data sets cover the period of 1951–2020, sunshine duration data are of different temporal coverage: from station Łódź, they cover the period of 1951–2020, from station Poznań, they cover 1959–2020, from stations Gorzów and Kalisz, they cover 1966–2020, and from stations Częstochowa and Koło, they cover 1972–2020. In all common observation periods, the solar radiation series show a high positive correlation.

The values of the monthly geopotential height at the level of 500 hPa were obtained from the NOAA NCEP-NCAR CDAS-1 MONTHLY Intrinsic Pressure Level phi: Geopotential height data collection. This is the Reanalysis Project collection [41]. In this study, the data were used on a profile located along the latitude of 52.5° N, between the longitudes of 10° W and 60° E, and with a resolution of 2.5°λ. From the same set, the values of the

atmospheric pressure time series at the sea level (hereinafter referred to as SLP—Sea Level Pressure; CDAS-1 MONTHLY Intrinsic MSL pressure: Pressure data) were obtained for the grid [52.5° N, 17.5° E]. This point is located in the central part of the WRC.

The time series of the air circulation indices used in this study include the annual frequency of the macrotypes of the mid-tropospheric circulation according to the Vangengeim–Girs classification [42,43]. Data on the frequency of macrotypes for the period from January 1951 to March 2018 were derived from the appendix to the paper of [44], while the remaining data, until December 2020, were obtained directly from AANIA (Arkticheskij and Antarkticheskij Nauchno-Issledovatel'skij Institut, Sankt Petersburg, RF).

2.2.2. North Atlantic (NA) Surface Temperature Data

The NA SST data were derived from ERSST v.5 (NOAA NCDC ERSST version5: Extended Reconstructed Sea Surface Temperature Dataset [45]). This is a global monthly data set with the spatial resolution of $2^\circ \times 2^\circ$. From this set, the time series of monthly SST values from January 1950 to December 2020 were collected in latitudinal profiles every 10° , from 20° N to 70° N, and every 10° at longitudes from the western to the eastern edge of the continents (37 series in total). From the monthly values, the series of annual SST values in individual grids were calculated as ordinary arithmetic averages in a calendar year. The “raw”, deliberately not processed (not converted into the SST anomalies, no trends removed, and no filtration performed) SST annual values were used in the calculations.

2.3. Methods

The number of days in a year with low flows on rivers in the WRC was adopted as a measure of the occurrence of hydrological droughts, as suggested by [9,46]. It can also be considered as one of the measures of the drought intensity in a given year, which is indicated by the number of days with low flows; the greater it is, the more intense and severe the hydrological drought recorded in the WRC in a given year is. Analyzing the sum of days with low flows in a year also enables such situations in which the hydrological drought occurred in two or more periods in a given year to be synthesized.

2.3.1. Low Flows as a Measure of Hydrological Droughts

The study analyzed the low flows below the threshold value, which was adopted as the 0.1 (10%)—(Q_{10}) percentile from the set of daily flows in the multi-annual period of 1951–2020. The low-flow periods were characterized with the use of the following parameters:

- number of days (T_{LF}) with flows below the threshold value (duration of low flows);
- volume of the low-flow runoff (V_{LF})—the volume (in m^3) of water flowing during the low-flow periods;
- water shortage in the low-flow period (V_{WS})—the volume of the shortage of water in m^3 ;
- theoretical volume of runoff (V_{Q10})—the water volume flowing during the low-flow periods below the threshold value Q_{10} ;
- coefficient of low-flow depth (CLFD [-]) determining the share of water shortage in the contractual limiting volume. The greater the value of the coefficient, the deeper the low flow ($CLFD = V_{WS}/V_{Q10}$).

2.3.2. Statistical Methods

Due to a significant number (14) of positively correlated series pertaining to the annual number of days with low flows (T_{LF}) in the WRC, they were subjected to PC (Principal Component) analysis. The PC method allowed us to reduce the number of variables and detect the main elements of the dataset structure. Two main statistically significant components in the series of the number of days with low flows were detected.

The eigenvectors of these components were then correlated with the annual SST series in each of the grids. The sets of correlation coefficients for the individual vectors

at the individual nodal points of the grid with specific coordinates were then processed into a graphical form as isocorrelate maps. The isocorrelate interpolation was performed automatically using the conventional kriging method.

Due to the large time scale of the relationships between the slowly changing thermal state of the ocean and the delayed reaction of the atmosphere, the analysis of the correlations between the SST and the eigenvectors was carried out using two temporal approaches: the first was asynchronous, in which the SST series (1950–2019) was preceded by one year of the eigenvector time series (1951–2020), and the second was synchronous, in which the SST series and the eigenvector time series were simultaneous (1951–2020). The two temporal approaches used in the analysis also aimed to explain the autocorrelations between the annual runoff of the Warta River and the course of the number of days with low flows in the WRC.

In order to establish the various types of detected relationships, in addition to the linear correlation analysis, forward stepwise regression analysis and analysis of variance were used. The forward stepwise regression is a variant of regression analysis [47], in which only statistically significant variables (predictors) are entered into the model.

In all calculations, $p = 0.05$ was assumed as the statistical significance limit, and $p = 0.001$ was assumed as the high statistical significance limit. The analysis was carried out for the period of 1951–2020. The length of this period (70 years) enables conclusions of a climatic nature to be drawn, and the length of the series ensures that the conclusions drawn from the statistical analyses have a solid formal basis. All calculations were performed using the statistical program STATISTICA PL, by StatSoft®. This package automatically calculates significance test values for a given type of statistical operation (t -tests, F -tests, etc.).

3. Results

3.1. Duration of Low Flows

Low flows (below Q_{10}) in the analyzed rivers in the period of 1961–2020 occurred in the number of 32 to 52 cases (years). The average number of days with flows below Q_{10} ranged from 48.2 (the Prosna River—the Bogusław gauge) to 78.8 (the Noteć River—the Pakość gauge). These values were clearly different in the two distinguished sub-periods. In the years 1988–2020, the number of days with low flows (T_{LF}) in most rivers increased to reach a maximum of 94.9 days (the Gaśawka River—the Żnin gauge). In the whole multi-annual period of 1951–2020, the increase in the number of days with low flows was statistically significant (Table 2, Figure 2). In the years 1951–1988, the number of low-pressure days was characterized by a downward trend, while in the years 1988–2020, it was characterized by an upward trend. In the studied rivers, the coefficient of low-flow depth (CLFD) also showed different values in the two sub-periods. The analysis shows that not only does the number of days with a low flow (T_{LF}) increase, but also that the runoff decreases, which causes the coefficient of low-flow depth (CLFD) to increase.

3.2. Principal Component (PC) Analysis

The PC analysis revealed, in the set of 14 time series for the number of low-flow days (T_{LF}), the existence of two main components with eigenvalues greater than 1.0. They explain 71.35% of the total variation in the number of days in a year with low flows in the years 1951–2020 in the set of 14 water gauges in the WRC. The first principal component with an eigenvalue of 8853 explained 61.87% of the total variance of the set, and the second, with an eigenvalue of 1197, explained 9.85% of this variance. The remaining principal components with eigenvalues lower than 1.0 were statistically insignificant, according to the Kaiser criterion. This was also confirmed by the “scree” test [47,48].

The time series of factor values 1 and 2 of the principal component formed the eigenvectors (Ev), which were analyzed. The course of both eigenvectors is shown in Figure 3. In the course of eigenvector 1, there was a weak and statistically insignificant positive trend ($0.0112 (\pm 0.0058)$ units·year⁻¹, $p = 0.058$). In the course of eigenvector 2, there was a

negative trend, twice as strong and statistically significant ($0.0225 (\pm 0.0053) \text{ units} \cdot \text{year}^{-1}$, $p < 0.001$).

Determining the values of 1Ev showed that these were standardized deviations from the average number of days with low flows in a year at all analyzed water gauges. This means that 1Ev is a standardized anomaly of the average number of days with lows in the WRC. There is a close relationship between the values of the eigenvector 1 series from k-year (independent variable, designated as 1Ev (k)) and the average number of days with a low flow in k-year (dependent variable, designated as T_{LF} (k)) (Equation (1)):

$$T_{LF} (k) = 34.592(\pm 0.239) + 37.343(\pm 0.241) \cdot 1Ev(k), \tag{1}$$

explaining 99.71% of the variance in the T_{LF} series in 1951–2020 ($R = 0.9986$, adj. $R^2 = 0.9971$, $F(1.68) = 24\,107$, $p \ll 0.001$, $SEE = 2.00$).

Table 2. Parameters of the low-flow periods in the analyzed rivers in the two sub-periods of the multi-annual period of 1951–2020. Numbering in accordance with Table 1.

No.	N	T_{LF}			T_{LF} Trend (Pearson's r) [-]			CLFD [-]		
		1951–2020	1951–1988	1988–2020	1951–2020	1951–1988	1988–2020	1951–2020	1951–1988	1988–2020
1	39	64.6	34.1	86.8	0.216	−0.607 ***	0.216	0.127	0.104	0.141
2	38	65.2	53.1	78.7	0.285 *	−0.648 ***	0.285	0.112	0.114	0.110
3	37	68.3	66.3	71.2	0.329 **	−0.611 ***	0.329	0.131	0.156	0.094
4	42	59.9	47.4	73.6	0.266 *	−0.451 **	0.266	0.106	0.086	0.129
5	46	55.4	44.3	66.5	0.228	−0.546 ***	0.228	0.154	0.145	0.164
6	52	48.2	39.2	57.3	0.390 ***	−0.497 **	0.390 *	0.153	0.139	0.168
7	41	60.0	53.5	65.6	0.310 **	−0.566 ***	0.310	0.265	0.316	0.220
8	46	52.8	55.7	50.3	0.400 ***	−0.112	0.400 *	0.263	0.247	0.277
9	39	65.2	48.2	81.4	0.163	−0.341 *	0.163	0.256	0.212	0.298
10	40	53.4	45.6	58.5	0.326 **	−0.435 **	0.326	0.316	0.256	0.356
11	40	58.0	43.6	71.0	0.450 ***	−0.357 *	0.450 **	0.272	0.241	0.300
12	32	78.8	72.3	82.8	−0.363 **	−0.059	−0.363 *	0.202	0.175	0.219
13	39	59.9	31.3	71.1	0.539 ***	−0.077	0.539 ***	0.304	0.248	0.326
14	34	73.6	43.1	94.9	0.595 ***	−0.171	0.595 ***	0.386	0.273	0.448

Note: N—number of years with low-flow periods in 1951–2020. Statistical significance of Pearson's r: *— $p < 0.05$, **— $p < 0.01$, ***— $p < 0.001$.

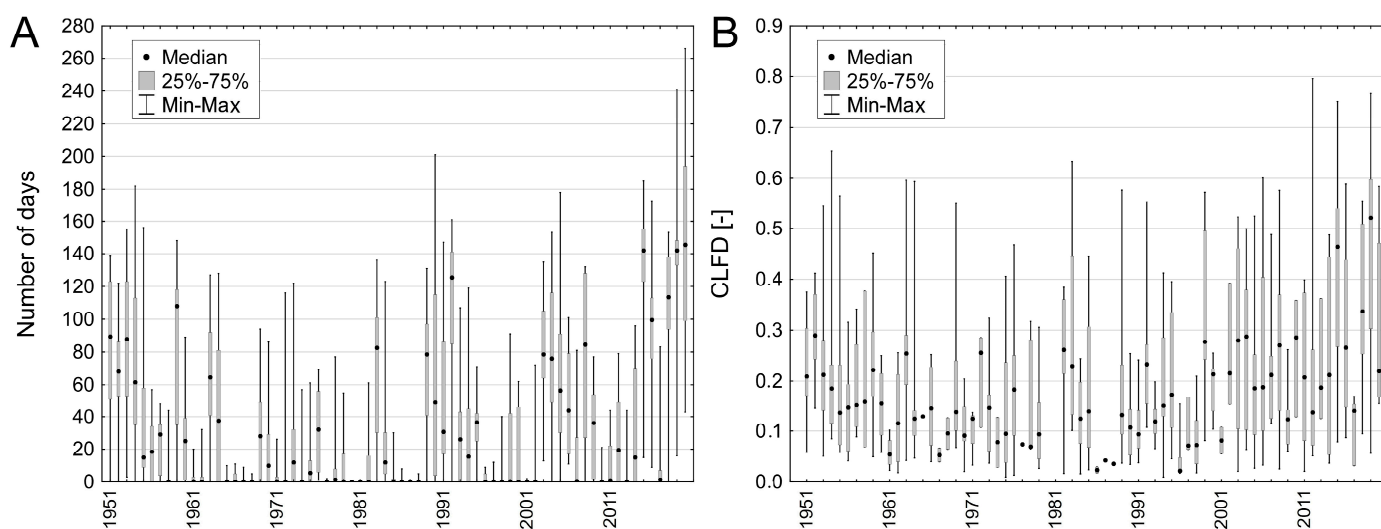


Figure 2. Number of days with low flows (A) and values of the coefficient of low-flow depth (B) in the Warta River catchment (WRC) in 1951–2020.

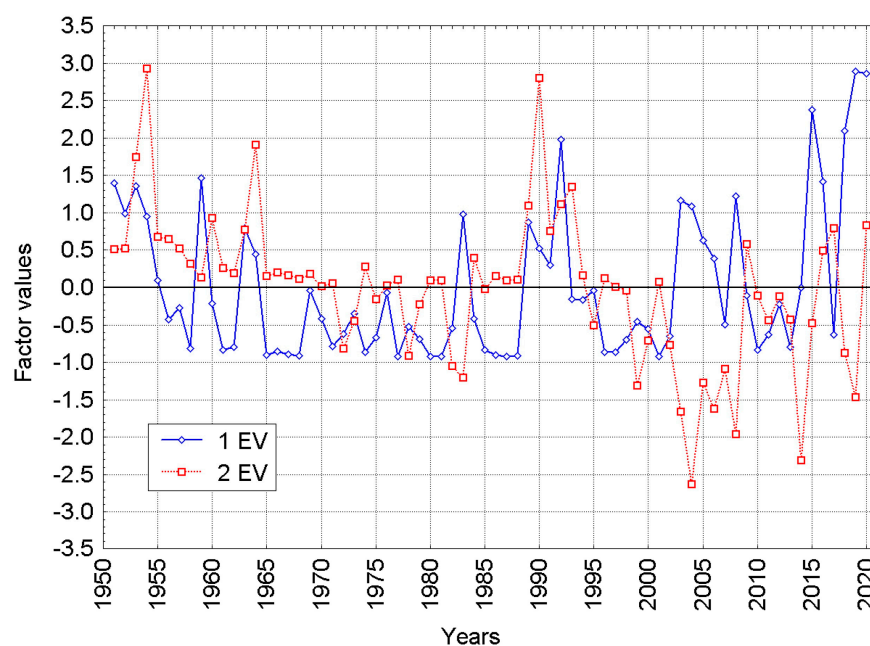


Figure 3. The course of the eigenvectors of the 1st and 2nd main component (1EV, 2EV) of a set of 14 water gauges with the number of days with low flows P 0.1 in a year in the Warta River catchment (WRC).

This vector shows a strong positive correlation with the average area annual air temperature in the WRC ($r = 0.51$ in the calendar year, and 0.48 in the hydrological year), while a strong negative correlation with the annual precipitation sum (r equal to 0.55 and -0.62 , respectively), which clearly indicates that the number of days with low flows in a year increases with the increase in the annual air temperature, and decreases with the increase in the average annual rainfall. As a result of this relationship, 1Ev shows a strong positive correlation with the de Martonne climate dryness index, the CDI [49], which includes the simultaneous influence of annual temperature and precipitation totals (Equation (2)):

$$CDI = P / (10 + T), \quad (2)$$

where P is the sum of annual precipitation (mm) and T is the annual temperature ($^{\circ}\text{C}$).

In this study, the CDI was calculated separately for the hydrological year (November–October) and the calendar year (January–December). Its correlation with 1Ev is strong and equal to -0.61 for the calendar year, and -0.73 for the hydrological year. The first vector is also highly significantly correlated with the CDI values from the previous hydrological year ($r = -0.46$, $p < 0.001$), which means that the T_{LF} in a given year not only depends on the course of the weather conditions in the same year, but also on the course of the weather conditions from the previous year. The regression analysis explains that 1Ev is a function of the CDI from two consecutive years, which altogether explain $\sim 52\%$ of the 1Ev variance (and the variability in the average number of days with low flows in the WRC in the analyzed 70-year period). The CDI from the previous year explains 5.1% , while that from the same year explains 47.5% of the 1Ev variance. This explains the reason for the occurrence of a relatively strong autocorrelation with an annual lag in the 1Ev series (partial autocorrelation coefficient equal to 0.468 , $p < 0.001$), and indicates the significant hydrological inertia of the WRC.

The physical sense of eigenvector 2 (2Ev) is not fully understood. The analysis shows that the series of 2Ev values are negatively correlated with the mean area annual temperature in the WRC (-0.33 ; $p = 0.007$ in the calendar year and -0.30 ; $p = 0.011$ in the hydrological year), but shows no relationship with the annual area sums of precipitation ($r = 0.08$ and 0.04 , respectively). This means that the value of this vector decreases as the temperature increases, but it does not respond to changes in the precipitation totals. The re-

relationships of 2Ev with the annual CDI are statistically insignificant, while the relationship in the current year is positive, and that with the CDI of the preceding year CDI is negative.

The analysis of the correlation between the series for the annual number of days with low flows at individual stations and the series of 2Ev values shows that the correlation signs change: at eight analyzed water gauges, these relationships are positive, and at six, they are negative. The strongest and most significant negative correlation coefficient values occur in these sub-catchments, in which the water gauge is located below large lakes (the Gařawa River—the Źnin gauge, the Mała Noteć River—the Gębice gauge). The distribution of stations in the common space of the first and second factor loadings seems to indicate that, apart from the first station (the Noteć River—the Pakość gauge), 2Ev reveals the spatially ordered, differentiated response of the catchment to changes in the weather conditions in a given year. This reaction varies depending on the physiographic conditions, mainly geological and geomorphological, that influence the nature of the river water supply; these encompass the land use, including forest cover. The Pakość gauge on the upper Noteć River, which strongly deviates from the others in terms of its response to changes in weather conditions, most likely experiences flows that are strongly distorted by the weir regulating the Noteć River flows below the Pakoskie Lake (Figure 4). Such an interpretation of the meaning of 2Ev seems to be confirmed by the cluster analysis, which was applied to the series of the number of days with low flows at individual water gauges (not presented here).

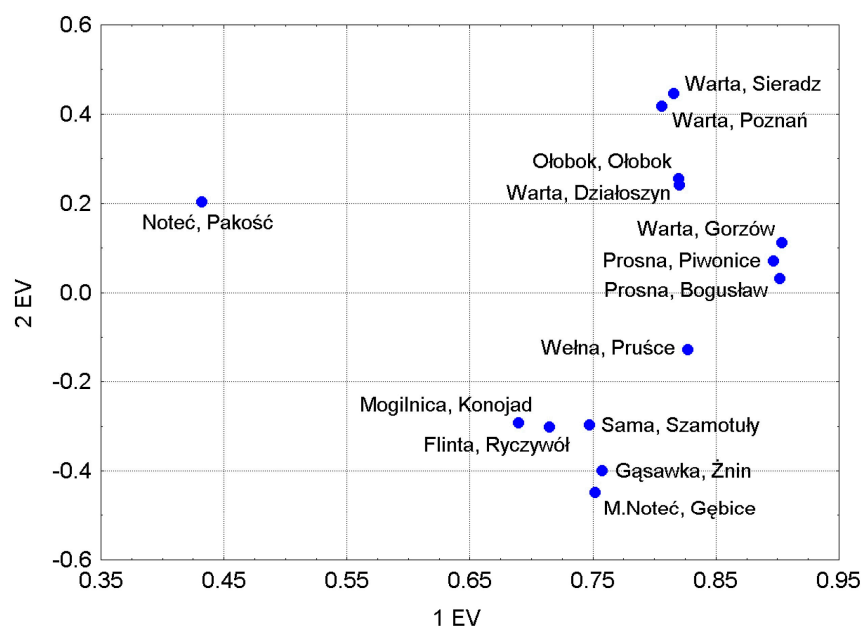


Figure 4. Location of the analyzed water gauges in the common space of 1Ev and 2Ev. The Pakość gauge on the Noteć River clearly differs from the other gauges. The rest of the gauges form two groups: group A: all gauges on the Warta River (Sieradz, Poznań, Działoszyn and Gorzów), on the Prosna River (Piwonice and Bogusław) and the Ołobok River (Ołobok), and group B: the Wełna River (Prušce), the Mogilnica River (Konojad), the Flinta River (Ryczywół), the Sama River (Szamotuły), the Gařawa River (Źnin) and the Mała Noteć River (Gębice). Group 1 is positively correlated, while group 2 is negatively correlated with 2Ev.

The variability in 1Ev is almost identical to the variability in the average number of days per year with low flows in the WRC and shows statistically significant relationships with meteorological elements; meanwhile, the physical meaning of 2Ev is not fully understood, and seems to show stronger relationships with factors other than meteorological conditions. Therefore, we will further present the results of the analysis of the relationship between the NA SST field and 1Ev, which explains more than half (about 62%) of the total variance in the number of days with low flows in the WRC.

3.3. Variability of NA SST and Hydrological Droughts

3.3.1. Relationship between the NA SST with the Number of Days with Low Flows

The analysis conducted of the asynchronous correlations between the SST series ahead in time and the time series of 1Ev indicates that the earlier spatial distribution of the annual NA SST value has a diversified impact on the T_{LE} in the WRC, taking place in the next hydrological year (Figure 5A). Since the cause must always precede the effect in time, it is obvious that earlier changes in the annual SST will condition the subsequent variation in the annual number of days with low flows.

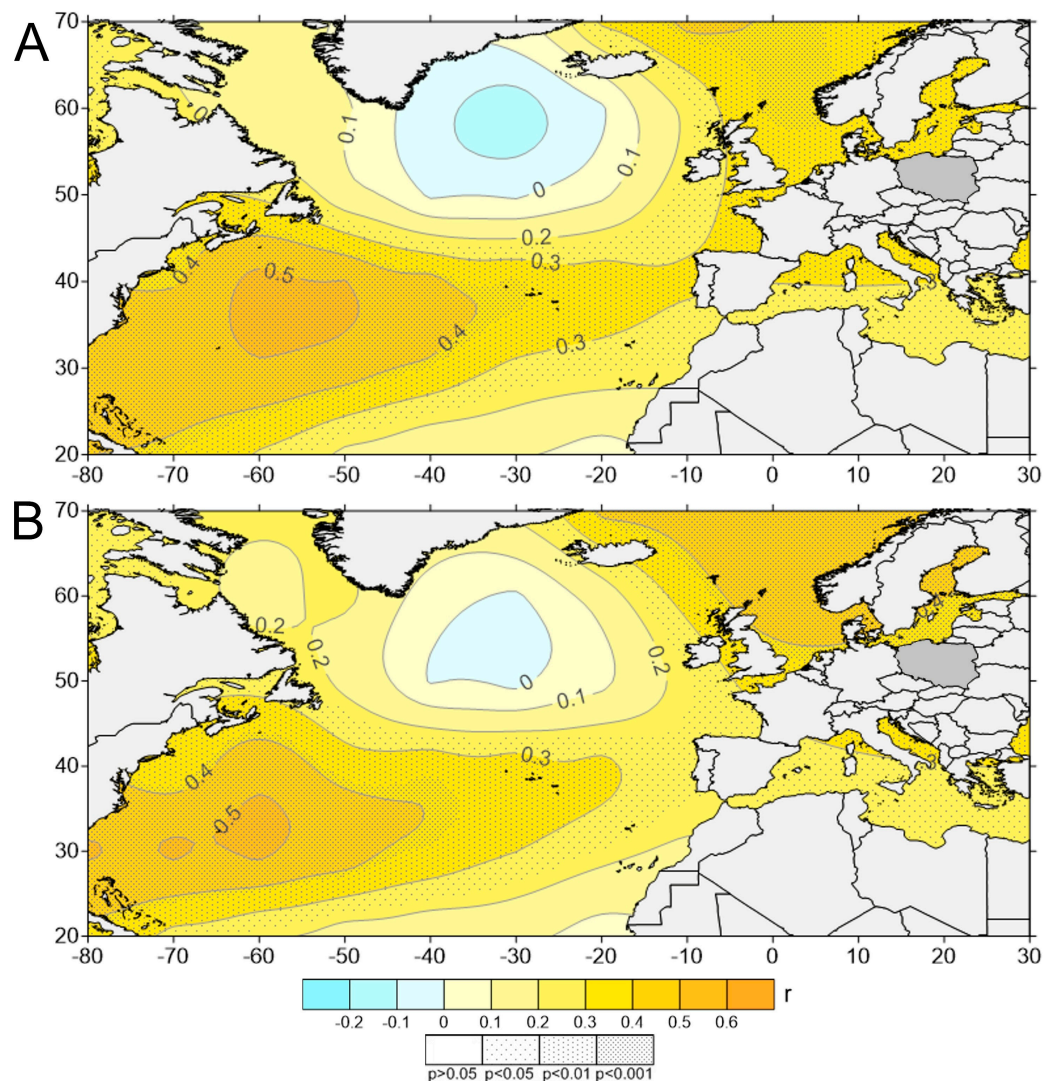


Figure 5. Asynchronous (A) and synchronous (B) correlation coefficients (r) between the annual SST in the grids and 1Ev of the number of days with low flows in the year in the Warta River catchment (WRC), and the level of their statistical significance (p) in the multi-annual period of 1951–2020.

Two areas are clearly visible in which there are clusters of positive correlation coefficients that are of weak and moderate strength (r ranging from 0.24 to 0.53), and are statistically significant and highly significant. The first of these are the waters lying in the north-eastern part of the NA, at the border of the waters of the temperate and subpolar zones [60–70° N, 10° W–10° E]. The maximum values of the correlation coefficients in this area of the Atlantic Ocean are 0.48 ($p < 0.001$), lying at 0° longitude and in latitudes 60–70° N. In terms of hydrology, both grids lie in the waters through which warm currents flow; at 60° N, 0° it is the terminal part of the North Atlantic Current, and at 70° N, 0° is the western branch of the warm Atlantic–Norwegian Current.

The second area of the Atlantic Ocean, much larger, consists of tropical and subtropical waters lying between 30 and 40° N. The maximum strength of the relationship between the SST variability and the subsequent changes in the T_{LE} is located at 30° N and 70–60° W ($r = 0.52$ – 0.53 ; $p < 0.001$). It is the western part of the NA, located at the center of the great circle of oceanic anti-cyclonal circulation. The grid [30° N, 70° W] lies in the center of the Sargasso Sea with very warm waters.

Areas with close to zero or negative, insignificant correlations [50–60° N, 40–30° W] are inside of the cyclonal circulation circle of the NA waters, with a weak upwelling; therefore, the course of the SST in that area shows a rhythm of changes distinct from the rest of the NA.

The spatial distribution of the values of the statistically significant asynchronous correlation coefficients (Figure 5A) indicates that it approximates the characteristics of the water dynamics of this part of the NA. The correlation coefficients are higher over warm waters, with an intense accumulation of solar energy, and the waters of warm currents that lead warmed and highly saline waters from the tropical zone of the western part of the ocean, through the subtropical temperate zones, to the Subarctic and Arctic (the North Atlantic and Atlantic–Norwegian currents).

The spatial distribution of the synchronous correlations (SST series and 1Ev series from the same years; 1951–2020; Figure 5B) is very similar to the spatial distribution of the asynchronous correlations.

The zone of the strongest correlations has shifted, compared to the previous state, from the region of tropical waters [30° N, 70–60° W] to the north-east, i.e., to the border of subtropical waters and the waters of the temperate zone of the NA [40° N, 60–50° W]. This shift corresponds to the shift of the water masses with the highest temperature and salinity under the influence of the THC NA. In the north, the strength of the relationships between the changes in the SST and 1Ev has definitely decreased, and the local maximum strength of the relationship has also been shifted.

The general conclusion from this analysis is that the NA SST changes show the spatially differentiated strength of the relationship with the occurrence of drought in the WRC. The conducted analysis made it possible to detect parts of the NA in which changes in the annual SST with a moderate strength ($r \sim 0.5$, $p < 0.001$), but with a very high degree of statistical significance, affect the length of the period with low flows in the WRC.

The spatial distributions of the correlation coefficients between the SST and the number of days with low water in the WRC reflect, in the generalized picture, some characteristics of the ocean dynamics—the spread of warm and heavily saline waters in the subsurface layer of the NA under the influence of current transmission. Thus, it can be concluded that the variability in the water dynamics of the NA has an impact on the frequency and intensity of hydrological droughts in the Greater Poland region.

The increase in the annual SST in the tropical waters of the western part of the NA in the region of ~30° N, 70–60° W indicates an increase in the probability of hydrological drought in the WRC in the next year, and the greater the SST increase is, the longer the duration of drought will be. The forward stepwise regression analysis showed that the changes in the annual SST in the grids [30° N, 60° W] and [30° N, 80° W] accounted for a total of 31% of the variance in the number of days with low flow (T_{LF}) in the following year ($y + 1$) (Equation (3)):

$$T_{LF(y+1)} = -1853.3(\pm 358.1) + 35.2(\pm 12.7) \cdot SST_{(y)}[30^\circ \text{ N}, 60^\circ \text{ W}] + 40.9(\pm 18.0) \cdot SST_{(y)}[30^\circ \text{ N}, 80^\circ \text{ W}] \quad (3)$$

In Equation (3), the SST variability in the grid [30° N, 60° W] explains 28.2% of the TLF variance, and the SST variability in the grid [30° N, 80° W] explains 5.1% of that variance. Equation (3) has a very large standard error of estimation (SEE), as many as 31 days. This shows that the prognostic usefulness of this formula is negligible, but it also clearly indicates (Figure 6) that changes in the SST in this part of the Atlantic Ocean have a

measurable effect on the size of the hydrological drought period in an area located more than 6500 km away from the Atlantic tropics.

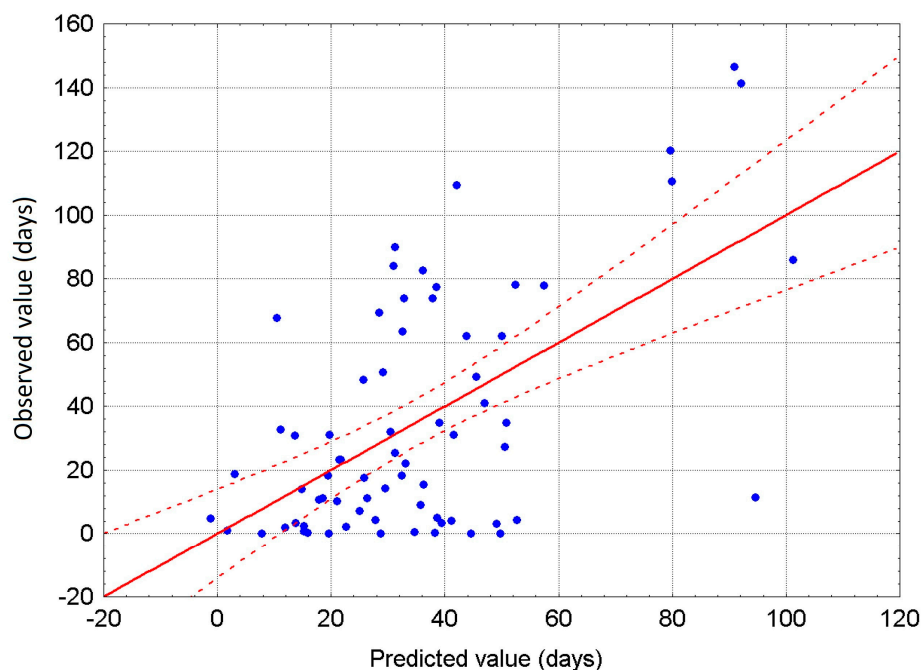


Figure 6. The predicted average number of days with low flows in the Warta River catchment (WRC) in a year, calculated using Equation (3), and the observed values.

3.3.2. Variability in the NA SST and the Course of the Annual Meteorological Elements

The analysis of the relationships between the SST and the number of days in a year experiencing the occurrence of hydrological drought in the WRC (T_{LF}) shows that the strongest and most significant relationships with the T_{LF} are shown by the variability in the SST in the tropical and subtropical waters on the western side of the NA. In the case of asynchronous correlations, it is the SST in the grid [30° N, 60° W] ($r = 0.53$), and in the case of synchronous correlations, it is the SST in the grid [40° N, 60° W] ($r = 0.54$). The differences in the values between these correlation coefficients (0.01) are statistically insignificant; it could be considered that the changes in the SST in both the asynchronous and synchronous correlations are related to the T_{LF} variability with the same strength.

The results of the analysis of the asynchronous and synchronous correlations between the SST variability in these grids and the annual area air temperature and annual area precipitation totals are summarized in Table 3.

Table 3. Correlation coefficients (r) between the annual SST in selected grids with the given coordinates and the annual area temperature (T) and the annual area precipitation totals (P) in the Warta River catchment (WRC), and their significance levels (p).

Grid	T		P	
	r	p	r	p
[30° N, 60° W] (a)	0.53	0.000	−0.04	0.736
[30° N, 60° W] (s)	0.67	0.000	−0.14	0.243
[40° N, 60° W] (a)	0.46	0.000	−0.10	0.395
[40° N, 60° W] (s)	0.61	0.000	−0.10	0.409

Note: a—asynchronous correlations: SST series from 1950–2019, T and P series from 1951–2020; s—synchronous correlations: SST, T and P series from the same years (1951–2020). Significance level $p = 0.000$ means that $p \ll 0.001$.

The presented data show that the variability in the air temperature of the WRC is strongly and significantly related to the SST variability, while there is no statistically significant relationship between the variability in the annual precipitation totals and the SST variability in the NA waters. The synchronous relationships between the SST and T are slightly stronger than the asynchronous ones, but both remain highly significant.

The analysis of the relationships between other climatic elements and the SST variability shows that these relationships are not limited to temperature. The values of the synchronous correlation coefficients between the SST in the aforementioned grids and other elements at the Poznań station, which among the stations located in the WRC is the closest to its center and has the most complete data series, provide a more detailed picture of these relationships (Table 4).

Table 4. Correlation coefficients (top row in the cell) and their significance levels (bottom row) between the annual SST in selected grids with the given coordinates and the annual general cloudiness (N), the annual relative humidity (F) and the annual sunshine duration (SD) at the Poznań station.

Grids	N (70 Years)	F (70 Years)	SD (62 Years)
[30° N, 60° W] (a)	0.14 $p = 0.258$	−0.45 $p = 0.000$	0.47 $p = 0.000$
[30° N, 60° W] (s)	0.04 $p = 0.732$	−0.48 $p = 0.000$	0.57 $p = 0.000$
[40° N, 60° W] (a)	0.17 $p = 0.155$	−0.32 $p = 0.006$	0.51 $p = 0.000$
[40° N, 60° W] (a)	0.06 $p = 0.649$	−0.40 $p = 0.001$	0.61 $p = 0.000$

Note: Correlation coefficients rounded to two decimals, p -values to three decimals. Significance level $p = 0.000$ means that $p \ll 0.001$. The correlated series of the annual sunshine duration (SD) cover only 62 years (1959–2020).

The SST correlations with the overall cloudiness (N) are insignificant, while the correlations with the relative humidity are of moderate strength, significant and highly significant. The negative sign of these correlations is consistent with the relationship between the humidity and temperature. Therefore, they may result from the temperature increase occurring over Poland due to the changes in the SST. As a result of the simultaneous increase in the temperature and decrease in the relative humidity, along with the increase in the SST, the field evaporation in the WRC increases. Estimated with the help of the N.N. method proposed by Ivanov (after [50]), the annual sums of field evaporation (Ev, mm) at the Poznań station are positively, relatively strongly and highly significantly correlated with the SST, both in asynchronous and synchronous relationships. The asynchronous correlation coefficient between the SST in the grid [30° N, 60° W] and the field pairing sums is 0.51, and the synchronous correlation is 0.57. This means that along with the increase in the SST in this area, field evaporation in the WRC also increases. With the increase in the SST in that part of the NA waters, an increase in the sunshine duration is also revealed (Table 4), which inevitably directly increases the temperature of the ground, which increases evaporation from its surface. Thus, the analysis of the relationships between the variability in the SST in the tropical and subtropical zones of the western part of the NA and the occurrence of hydrological droughts in the WRC gives a coherent picture, indicating that the main reason for the decrease in the value of the water balance in this area is the increase in water losses via evaporation. Weak and insignificant relationships between the SST variability and the annual area precipitation (Table 3) suggest that the SST has a minimal or no effect on the differentiation of precipitation totals.

A more detailed analysis corrects this view, taking into account the influence of the SST in the region of [30–40° N, 60–50° W] on the behavior of the geopotential height over Europe, and thus on the atmospheric circulation. The increase in the SST in this region leads to a relatively strong and highly significant increase in the height of the isobaric surface of 500 hPa (hereinafter referred to as h500) over Europe, including Central Europe.

An example of such positive correlations between the annual SST in the grid [30° N, 60° W] and h500 at 52.5° N, 17.5° E, located over the north-eastern part of the WRC ($r = 0.58$, $p < 0.001$), is shown in Figure 7. This figure confirms that an increase in the SST above 24.4–24.5° C in the grid [40° N, 60° W] results in a strong increase in the h500 over the WRC.

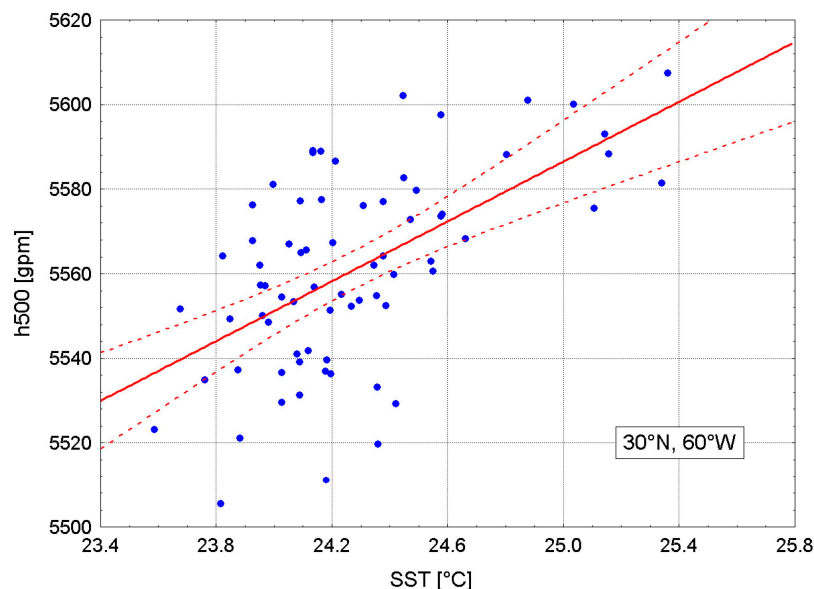


Figure 7. Relationship between the annual SST in the grid [30° N, 60° W] and the geopotential height of 500 hPa (h500) at the point [52.5° N, 17.5° E], located over the NE part of the Warta River catchment (WRC).

The variability in the geopotential height at this point in the WRC is highly significantly correlated both with the average annual area air temperature and, to a lesser extent, the average annual area sum of precipitation ($r = 0.79$ and -0.42 , respectively). There is also a strong and highly significant correlation between the h500 and the sea level atmospheric pressure at the same point, from which the geopotential height data were derived ($r = 0.70$).

A more complete picture of the effects of the change in the height of the geopotential under the influence of the SST changes in the Atlantic tropics and subtropics is provided by the overview of the correlation coefficients between the annual height of the h500 and the climatic elements measured at the Poznań meteorological station (Table 5).

Table 5. Correlation coefficients between the annual height of the geopotential at the level of 500 hPa at [52.5° N, 17.5° E] and the annual climatic elements measured at the Poznań station ([52.25° N, 16.50° E], 86 m a.s.l.): atmospheric pressure at sea level (SLP), air temperature (T), precipitation totals (P), total cloudiness (N), relative humidity (F) and sunshine duration (SD). Correlations of h500 with SLP, T, P, N and F from the years 1951–2020, with SD from the years 1959–2020.

SLP	T	P	N	F	SD
0.72	0.78	-0.30	-0.48	-0.70	0.77
$p = 0.000$	$p = 0.000$	$p = 0.011$	$p = 0.000$	$p = 0.000$	$p = 0.000$

The correlation coefficients between the variability in the h500 and climatic elements presented in Table 5 confirm that the SLP, T and SD increase with the increase in the h500, and at the same time, the total cloudiness, relative humidity and total precipitation decrease. This type of dependence is shaped at the level of weather conditions, i.e., processes of a synoptic scale.

The average annual atmospheric pressure over an area (point) in temperate latitudes is a function of the number of low-pressure systems passing over it during the year and the

pressure prevailing in them. The more such systems move over a given area in a year and the lower the pressure in them, the lower the average annual pressure will be. Since the year has a finite number of days, a decrease in the number of low-pressure systems passing over a given area during the year will necessarily result in an increase in pressure.

The increase in the annual geopotential height entails a statistically significant increase in pressure (Table 5). This means that along with the increase in the h500 over the WRC, the frequency of low-pressure (cyclonic) systems decreases during the year, and thus the share of anticyclonic situations must increase. In other words, as the SST increases in the Atlantic tropics, the h500 increases over Central Europe (and thus over the WRC) (Figure 7), and so does the atmospheric pressure (Table 5). This indicates an increase in the frequency of synoptic anticyclonic situations, and at the same time, a decrease in the frequency of cyclonic situations over the WRC along with an increase in the SST in the Atlantic tropics and subtropics.

Thus, with the increase in the SST in the Atlantic tropics and subtropics, the share of low-pressure weather decreases, while the share of anticyclonic weather over Central Europe increases during the year. The occurrence of atmospheric fronts is typical for low-pressure weather. In frontal weather, there are extensive areas of layered cloud cover, limiting the inflow of solar radiation to the surface and bringing prolonged rainfall of varying intensity. Anticyclonic weather is characterized by clear skies or low cloud cover, a decrease in precipitation totals, an increase in sunshine duration and air temperature in the warm half-year, and a decrease in the relative humidity. An increased frequency of this type of “high-pressure” (anticyclonic) weather not only increases evaporation, but also reduces the frequency of long-term frontal precipitation (Table 5).

As a result of these dependencies, changes in the geopotential height at the level of 500 hPa over the WRC (at 52.5° N, 17.5° N) are significantly positively correlated with 1Ev of the number of days per year experiencing hydrological drought ($r = 0.47, p < 0.001$) and the annual evaporation (Ev; $r = 0.77, p < 0.001$), and negatively correlated with the annual number of days with precipitation ≥ 1.0 mm ($r = -0.60, p < 0.001$) and the annual CDI ($r = -0.49, p < 0.001$). The latter indicates an increase in “climate aridity” with an increase in the annual h500.

The correlation between the SST in the western part of the tropical and subtropical NA and the geopotential height over Europe demonstrates that changes in the SST in this basin are also an indirect cause of changes in the precipitation totals over the WRC and changes in cloud cover. With the increase in the SST in the Atlantic tropics, the values of these climatic elements decrease, and therefore the probability of droughts increases.

3.3.3. Mechanism of the Influence of the NA SST Variability on the Occurrence of Hydrological Droughts

The main question asks how the mechanisms that make changes in the SST in the Atlantic tropics lead to weather changes over Central Europe, which then regulate the variability of the river flow regime, work. The key issue is to explain the relationships between the variability in the SST over the Atlantic and the changes in the height of the geopotential over Central Europe, because the mere occurrence of even significant correlations between these values does not prove the existence of causal relationships between them.

The spatial distribution of heat resources in the NA waters, through the size and location of heat flows from the ocean to the atmosphere, determines the characteristics of the middle-tropospheric circulation (500 hPa). One of the manifestations of the distribution of heat resources in the ocean waters is the spatial distribution of the SST. Reservoirs in which the waters contain greater than average heat resources may transfer increased amounts of heat to the atmosphere, and with average sizes of heat fluxes from the ocean to the atmosphere, they may function for longer than with the average heat resources. Changes in the location of heat flows from the ocean to the atmosphere and their intensity entail corresponding changes in the meridional thermal gradients in the mid-troposphere, thus

affecting the wave number and arrangement of long waves (the Rossby waves) traveling over the ocean and then over those extending over the areas of continents east of the ocean.

A long wave is formed by a system of interrelated upper wedges and upper troughs that move through space or may periodically form a standing wave. In the Atlantic–Eurasian circulation sector [70° W–110° E], the Vangengeim–Girs classification [42,43] distinguishes three basic forms (macrotypes) of long-wave arrangement, depending on their length (wave number) and the geographical distribution of the upper wedges and upper troughs. The forms of the arrangement of the long waves are W (wave number 4, smaller wave amplitude), and E and C (wave number 5, larger wave amplitudes). The occurrence of macrotype W forces strong zonal circulation in the middle and lower troposphere. The occurrence of macrotypes E and C forces a meridional circulation, but in each of these macrotypes, different positions of air streams are directed to the south and north.

Each of these macrotypes is characterized by the specific geographic location of the upper wedges and upper troughs, related to the baric systems functioning in the lower troposphere (850–1000 hPa). As a result, the macrotype occurring during a given day determines the weather processes over a given area [51,52]. These issues are presented in more detail in the paper of [28].

The occurrence frequency (number of days in a year) of macrotypes W and E is related to the SST variability in the Atlantic tropics, while the frequency of macrotype C shows no correlation with changes in the thermal state of the NA. The SST increase in the Atlantic tropics and in the north-eastern part of the NA entails an increase in the frequency of macrotype W and, at the same time, a decrease in macrotype E. It has to be pointed out that the number of days in a year is constant, and during a given day, there may be only one macrotype. As a result, an increase in the frequency by one day of one macrotype form must entail a one-day decline in the frequency of one of the other two macrotypes. There is a very strong negative correlation between the annual frequency of macrotypes W and E (−0.83; 1951–2020).

In the case of the annual SST in the grid [30° N, 60° W], its variability is correlated with the annual frequency of macrotype W at the level of 0.44 ($p \ll 0.001$) and with the frequency of macrotype E at −0.35 ($p = 0.003$); however, the SST in only one $2 \times 2^\circ$ grid does not give a fuller insight into the real impact of SST changes on the mid-tropospheric circulation. A more complete picture can be obtained by averaging the SST over a larger water body. The average SST from the grids [30°–40° N, 50–60° W] (hereinafter referred to as SST_{NAWT} variable; North Atlantic—West Tropic) shows a correlation with the frequency of macrotype W at the level of 0.53 (Figure 8), and with the frequency of macrotype E at the level of 0.35 (both $p < 0.001$). This means that the occurrence of a temperature higher than the long-term average of the surface of the North Atlantic in the tropical and subtropical zones to the west of 40° W is favorable to the occurrence of a strong zonal circulation over Europe. The same SST variability in the indicated area shows the same strong correlation ($r = 0.53$, $p < 0.001$) with the number of days experiencing low flows in the WRC (Figure 9).

Since the upper wedges and upper troughs are nothing else than the elevated or lowered geopotential surfaces over a given area, the existence of relations between the SST variability in a given area and the variability in the geopotential height at any level, for example, the 500 hPa (h500) at any point, can be detected by a simple correlation between the SST and h500. These relationships in space should have a wave character (reproduce successive increases and decreases in the height of the geopotential with the change in the SST in space); therefore, it is most advisable to study them along latitudinal profiles. An example of such an analysis is presented in Figure 10A, which is a graphical representation of the distribution of correlation coefficients between the annual SST in several grids located in the Atlantic tropics (30° N: 70° W, 60° W and 50° W; see the map—Figure 5), and h500 at the parallel of 52.5° N, along the longitudes between 10° W and 60° E (Figure 10B). This profile runs through Europe, from Ireland to the western part of Kazakhstan, and crosses at longitude ~15.5–19° E the area of the WRC.

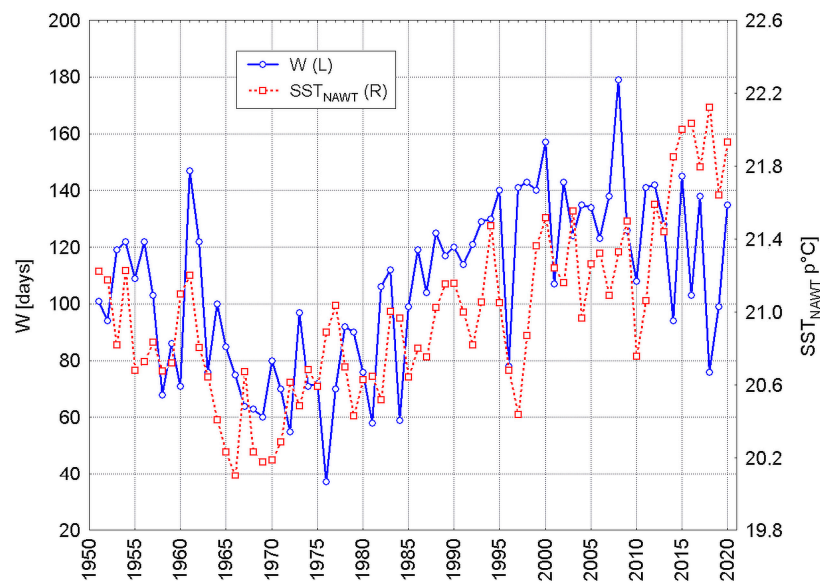


Figure 8. The course of the annual frequency of macrotype W according to the Vangengeim–Girs classification (W) and the annual SST in the western part of the Atlantic tropics (SST_{NAWT}).

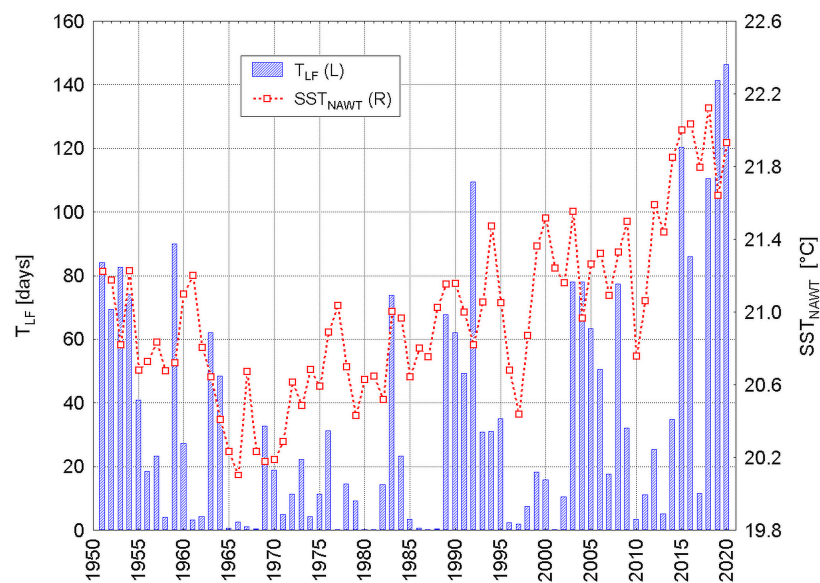


Figure 9. The course of the average number of days per year experiencing low flows in the WRC (T_{LF}) and the annual SST in the western part of the Atlantic tropics (SST_{NAWT}).

The correlation coefficients between the SST and h500 at individual longitudes smoothly change their values; starting from 10° W, they increase to 20–25° E and then decrease, reaching their minimum already beyond the profile boundary. Between the longitudes ~0° and ~40° E, these correlations are highly significant. Such an arrangement recreates the arrangement of a long wave, with the upper wedge axis located between 20 and 25° E. Since the sign of the correlation coefficient is positive, it becomes evident that an increase in the SST in any of these grids must imply the strongest increase in the h500 only in the longitude zone of 20–25° E.

Since the h500 is strongly and highly significantly correlated with the SLP (see Table 5), there should also be a direct relationship between the values of the h500 at individual longitudes and the series of eigenvector 1 for the number of days experiencing drought in the WRC. The verification of this hypothesis is confirmed in Figure 10B.

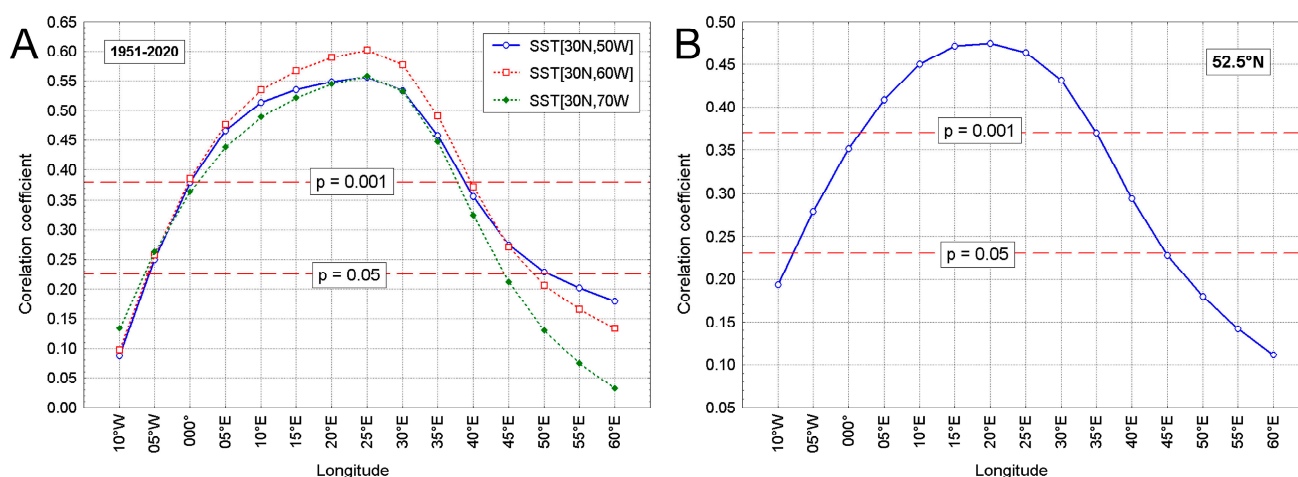


Figure 10. Distribution of correlation coefficients (r) between (A) the annual geopotential height at 500 hPa (h_{500}) and the annual SST from the tropical region (30° N) of the western North Atlantic (NA) (longitudes 70 , 60 and 50° W), (B) the annual geopotential height at 500 hPa at latitude 52.5° N, longitudes from 10° W to 60° E and an eigenvector 1 for the number of days experiencing hydrological drought in a year in the Warta River catchment (WRC) in 1951–2020. Marked are significance levels $p = 0.05$ and $p = 0.001$.

The examples presented in Figure 10A,B prove that the SST changes, by influencing the regulation of the long wave position, in this case the location of the upper wedge, the height of the geopotential over areas that are far from the ocean.

Thus, the SST variability in the Atlantic tropics and subtropics determines, in a significant percentage, the variability in climatic elements over Europe and Poland and a number of other processes and phenomena, including the occurrence of hydrological droughts.

4. Discussion

The presented relations between the SST and the number of days in a year experiencing low flows result from the influence of SST changes on changes in the atmospheric circulation. The increase in the SST in the Atlantic tropics entails an increase in the frequency of the Vangengeim–Girs macrotype W (Figure 8), and a simultaneous decrease in the frequency of macrotype E. The effect of this is that during periods of SST values that are higher than average in the Atlantic tropics, there is an increase in the frequency of macrotype W episodes and/or the prolongation of the series of days experiencing the occurrence of this macrotype. In these periods, the h_{500} and SLP increase over the WRC (and in general over Central Europe), and the frequency and duration of anticyclonic weather episodes increase, while the share of frontal weather events decreases.

In the system of the large-scale pressure field (SLP), the occurrence of macrotype W is associated with the strong eastward development of the wedge of the Azores High and the shift of the longer axis of that High to the north [53,54]. This is caused by an increase in pressure over Western and Central Europe in 45 – 55° N, and a shift in the tracks of low-pressure systems to higher latitudes, namely 60 – 70° N. This means that an increase in the intensity of the zonal circulation is conducive to the occurrence of droughts in the WRC. This formulation can be extended to the whole area of the Polish Lowlands and other parts of Poland [55,56], and probably the whole of Central Europe.

The relationships between the T_{LF} and the SST field in the North Atlantic are not very strong, and in a number of cases, there is no consistency between the SST and T_{LF} (see Figure 9; e.g., 1961, 1999–2002) when periods of high SST correspond to low T_{LF} . This lack of a close relationship can be explained by the joint action of several factors at the same time. There seem to be two main factors: one of them is the meteorological factor, namely the duration of episodes seeing the occurrence of macrotype W, i.e., the number of days experiencing the uninterrupted occurrence of this macrotype. According to Degirmendžić

and Kożuchowski [57], the most common multi-annual average duration of an episode of macrotype W is six days. In years with high SST values in the Atlantic tropics, the length of episodes of this macrotype can vary significantly. In years when the duration of episodes of macrotype W are shorter or close to average and relatively evenly distributed over time, low flows of a longer duration do not occur. Only the longer episodes of the occurrence of macrotype W, usually lasting consecutively for more than nine days and preceded by shorter episodes, result in a low flow.

The second factor causing the weakening of the relationships between the NA SST and T_{LF} is the geological structure of the WRC, which is situated in post-glacial areas, predominantly built upon permeable rocks. Consequently, the WRC rivers are largely fed by groundwater. In such conditions, retention plays an important role in the formation and course of low flows. Groundwater retention will be significant if, in the preceding year, precipitation is clearly higher than average and weather conditions are not conducive to large water losses caused by evaporation. An increase in the frequency of anticyclonic weather in the following year will not lead to a long-lasting low flow, as its beginning will be delayed. Unfortunately, the same factor leads to a decrease in groundwater retention, resulting from increased evaporation, and the occurrence of an increasingly longer series of successive years experiencing hydrological droughts in the WRC and deepening low flows (Figure 2B) after 1988.

The conclusions presented in this paper clearly differ from the results of the research conducted by [1], who determined that the observed increase in the frequency of droughts in Eastern Europe (Romania) was associated with the transition from the zonal to meridional circulation around the year 1850. It should be noted that macrotype W is a form of zonal circulation and it also forces zonal lower circulation [43,44,57,58]. In 1951–1988, there were periods of strong meridional circulation (E + C and E) [59]. From 1988–1989, the zonal circulation epoch W began [59], in which the attendance of the zonal macrotype W increased on average by more than 20 days per year in relation to the long-term average, and the attendance of the meridional macrotype E decreased by approximately the same number of days. From that moment on, the downward trend observed in the number of days experiencing low flows in the WRC ended and an upward trend began, one that was statistically significant in 2020 (see Section 3.1., Table 2).

There is also a fundamental difference between the results of our study and the findings of [26], which investigated the relationships between the SST in the North Atlantic and droughts in Europe with a 1000-year perspective. They concluded that droughts, and especially mega-droughts, occurred in the conditions of a “cold” ocean. In fact, it is difficult to compare and discuss at this point the results of research conducted on the millennium time scale, based mainly on various types of reconstructions, with the results of a study based on real data from 70 years of the multi-annual period of 1951–2020. In our study, the analysis of the mechanism involved in hydrological drought formation and the obtained results (see e.g., Figure 8) indicate that one of the most important causes of this multi-faceted phenomenon is the “warm” North Atlantic. Although there is no close relationship between the SST in the Atlantic tropics (variable SST_{NAWT}) and the number of days experiencing hydrological drought in the WRC, with changes in the SST_{NAWT} explaining about 30% of the T_{FL} variance, it can be seen (Figure 9) that changes in the SST in the Atlantic tropics lead to long-term changes to the number of days experiencing hydrological drought in the WRC.

While the findings of our study shed new light on the relationships between the thermal state of the North Atlantic and droughts in Central Europe, the limitations of this research have to be underlined. The first one is related to the fact that the analysis of the relationships between the SST and the number of days experiencing hydrological drought in the WRC was carried out at a low spatial resolution. This resulted in a generalized picture of the spatial distribution of isocorrelates. Other limitations are related to the data resolution (grid vs. point-station) and the differences in the data sources used in our study. As a result, while this research makes it possible to indicate areas in which such relations

occur, it certainly does not enable the points at which these relations reach both their maximum and minimum to be indicated. For this reason, the values of the correlation coefficients between the SST and the number of days with low flows presented in this research should be considered as the first approximation, similar to the indicated locations of their extreme values.

5. Conclusions

This study revealed an increasing number of days with deep low flows in the WRC, the third largest river basin in Poland. It was determined that the extended periods of hydrological drought in that area were related to a strong increase in the SST in the tropical and subtropical North Atlantic.

Sutton and Hodson [14] examined the relationships between the thermal state of the North Atlantic and the summer temperature in Europe, and concluded that as long as the North Atlantic remained anomalously warm, the climatic pattern of summer in Europe, i.e., the coexistence of anomalously mild, wet summers in Northern Europe and hot, dry summers in Southern Europe, would continue. The results of the present research allow us to extend these findings: as long as the western, tropical part of the NA remains anomalously warm, hydrological droughts will continue and deepen in Central Europe, and perhaps also in Western Europe. The increase in the SST in that part of the NA, observed since the 1990s, is not positive for water management in large parts of Europe. The temperature of the tropical NA waters has risen sharply since 2000, and this process has been accelerated since 2014. In 2022, the SST reached unprecedentedly high values in that area. Considering the mechanisms involved in the changes in heat resources in ocean waters, it is unlikely that the SST in the tropical Atlantic will decrease rapidly in the next few years. This indicates the very high probability of the occurrence of extreme hydrological droughts persisting in Central Europe, and probably also in Western Europe.

Author Contributions: Conceptualization, A.A.M., A.S. and D.W.; methodology, A.A.M., A.S. and D.W.; software, A.A.M., L.S., A.S. and D.W.; validation, A.A.M., A.S. and D.W.; formal analysis, A.A.M., A.S. and D.W.; investigation, A.A.M., A.S. and D.W.; data curation, A.A.M., A.S. and D.W.; writing—original draft preparation, A.A.M., L.S., A.S. and D.W.; writing—review and editing, L.S.; visualization, A.A.M., A.S., D.W. and A.P.; supervision, L.S. and D.W. All authors have read and agreed to the published version of the manuscript.

Funding: This research was carried out under the internal research grant (internal faculty research grant) at the Faculty of Geographical and Geological Sciences of Adam Mickiewicz University in Poznań, Poland.

Data Availability Statement: The data presented in this study are available upon request from the corresponding author.

Conflicts of Interest: The authors declare no conflict of interest.

References

1. Nagavciuc, V.; Ionita, M.; Kern, Z.; McCarroll, D.; Popa, L. A ~700 years perspective on the 21st century drying in the eastern part of Europe based on $\delta^{18}\text{O}$ in tree ring cellulose. *Commun. Earth Environ.* **2022**, *3*, 277. [[CrossRef](#)]
2. Ionita, M.; Nagavciuc, V.; Scholz, P.; Dima, M. Long-term drought intensification over Europe driven by the weakening trend of the Atlantic Meridional Overturning Circulation. *J. Hydrol. Reg. Stud.* **2022**, *42*, 101176. [[CrossRef](#)]
3. Conradt, T.; Engelhardt, H.; Menz, C.; Vicente-Serrano, S.M.; Farizo, B.A.; Peña-Angulo, D.; Domínguez-Castro, F.; Eklundh, L.; Jin, H.; Boincean, B.; et al. Cross-sectoral impacts of the 2018–2019 Central European drought and climate resilience in the German part of the Elbe River basin. *Reg. Environ. Chang.* **2023**, *23*, 32. [[CrossRef](#)]
4. Lorenc, H. Climatological and meteorological extremes in Poland in relation to the 5th IPCC Report. In *Klimat a Społeczeństwo i Gospodarka*; Lorenc, H., Ustrnul, Z., Eds.; Wyd. PT Geofizyczne i IMGW-PIB: Warsaw, Poland, 2015; pp. 31–51. (In Polish)
5. Łabędzki, L. Problems of droughts in Poland. *Woda-Sr.-Obsz. Wiej.* **2004**, *4*, 47–76. (In Polish)
6. World Meteorological Organization (WMO); Global Water Partnership (GWP). *Handbook of Drought Indicators and Indices*; Svoboda, M., Fuchs, B.A., Eds.; Integrated Drought Management Tools and Guidelines Series 2; Integrated Drought Management Programme (IDMP): Geneva, Switzerland, 2016.

7. Doroszewski, A.; Józwicki, T.; Wróblewska, E.; Kozyra, K. *Agricultural Drought in Poland in the Years 1061–2010*; IUNG: Puławy, Poland, 2014; pp. 1–144. (In Polish)
8. Kaznowska, E. Characteristics of hydrological droughts on the example of selected rivers in the north-eastern part of Poland. *Infrastrukt. i Ekol. Teren. Wiej.* **2006**, *4*, 51–59. (In Polish)
9. Tokarczyk, T. *Low Water as an Indicator of Hydrological Drought*; Monografie Instytutu Meteorologii i Gospodarki Wodnej: Warsaw, Poland, 2010. (In Polish)
10. Węglarczyk, S. The definition criteria of the low flow and their influence on the characteristics of the low flow. 1. Stationarity of low flows. *Infrastrukt. i Ekol. Teren. Wiej.* **2014**, *II/1*, 251–263. (In Polish) [[CrossRef](#)]
11. Kushnir, Y. Interdecadal Variations in North Atlantic Sea Surface Temperature and Associated Atmospheric Conditions. *J. Clim.* **1994**, *7*, 141–157. [[CrossRef](#)]
12. Enfield, D.B.; Mestas-Nuñez, A.M.; Trimble, P.J. The Atlantic multidecadal oscillation and its relation to rainfall and river flows in the continental US. *Geophys. Res. Lett.* **2001**, *28*, 2077–2080. [[CrossRef](#)]
13. Park, W.; Latif, M. Ocean Dynamics and Nature of Air-Sea Interactions over the North Atlantic at Decadal Time Scales. *J. Clim.* **2005**, *18*, 982–995. [[CrossRef](#)]
14. Sutton, R.T.; Hodson, D.L.R. Atlantic Ocean forcing of North American and European summer climate. *Science* **2005**, *309*, 115–118. [[CrossRef](#)]
15. Pohlmann, H.; Sienz, F.; Latif, M. Influence of the Multidecadal Atlantic Meridional Overturning Circulation Variability on European Climate. *J. Clim.* **2006**, *19*, 6062–6967. [[CrossRef](#)]
16. Feng, S.; Oglesby, R.J.; Rowe, C.M.; Loope, D.B.; Hu, Q. Atlantic and Pacific SST influences on Medieval drought in North America simulated by the Community Atmospheric Model. *J. Geophys. Res.* **2008**, *113*, 1–14. [[CrossRef](#)]
17. Feng, S.; Hu, Q.; Oglesby, R.J. Influence of Atlantic sea surface temperatures on persistent drought in North America. *Clim. Dyn.* **2011**, *37*, 569–586. [[CrossRef](#)]
18. Sutton, R.T.; Dong, B. Atlantic Ocean influence on a shift in European climate in the 1990s. *Nat. Geosci.* **2012**, *5*, 788–792. [[CrossRef](#)]
19. Kushnir, Y.; Seager, R.; Ting, M.; Naik, N.; Nakamura, J. Mechanism of Tropical Atlantic SST Influence of North American Precipitation Index Variability. *J. Clim.* **2010**, *23*, 5610–5628. [[CrossRef](#)]
20. Delworth, T.L.; Zeng, F.; Vecchi, G.A.; Yang, X.; Zhang, L.; Zhang, R. The North Atlantic Oscillation as a driver climate change in the Northern Hemisphere. *Nat. Geosci.* **2016**, *9*, 509–513. [[CrossRef](#)]
21. Årthun, M.; Edelvik, T.; Viste, E.; Drange, H.; Fuervik, T.; Johnson, H.L.; Keenlyside, N.S. Skillful prediction of northern climate provided by the ocean. *Nat. Commun.* **2017**, *8*, 15875. [[CrossRef](#)] [[PubMed](#)]
22. Vigaud, N.; Ting, M.; Lee, D.-E.; Barnston, A.G.; Kushnir, Y. Multiscale Variability in North American Summer Maximum Temperatures and Modulations from the North Atlantic Simulated by an AGCM. *J. Clim.* **2018**, *31*, 2549–2562. [[CrossRef](#)]
23. Vicente-Serano, S.M.; Garcia-Herrera, R.; Barriopedro, D.; Azorin-Molina, C.; Lopez-Morena, J.I.; Martin-Hernandez, N.; Tomas-Burgera, M.; Gimeno, L.; Nieto, R. The Westerly Index as complementary indicator of the North Atlantic oscillation in explaining drought variability across Europe. *Clim. Dyn.* **2016**, *47*, 845–863. [[CrossRef](#)]
24. Ossó, A.; Sutton, R.; Shaffrey, L.; Dong, B. Observational evidence of European summer weather patterns predictable from spring. *Proc. Natl. Acad. Sci. USA* **2018**, *115*, 59–63. [[CrossRef](#)]
25. Svensson, C.; Hannaford, J. Oceanic conditions associated with Euro-Atlantic high pressure and UK drought. *Environ. Res. Commun.* **2019**, *1*, 101001. [[CrossRef](#)]
26. Ionita, M.; Dima, M.; Nagavciuc, V.; Scholz, P.; Lohmann, G. Past megadroughts in central Europe were longer, more severe and less warm than modern droughts. *Commun. Earth Environ.* **2021**, *2*, 61. [[CrossRef](#)]
27. Marsz, A.A.; Styszyńska, A.; Krawczyk, E.W. The log-term fluctuations in annual flows rivers in Poland and their relationship with the North Atlantic Thermohaline Circulation. *Przegląd Geogr.* **2016**, *88*, 295–316. [[CrossRef](#)]
28. Wrzesiński, D.; Marsz, A.A.; Styszyńska, A.; Sobkowiak, L. Effect of the North Atlantic Thermohaline Circulation on Changes in Climatic Conditions and River Flow in Poland. *Water* **2019**, *11*, 1622. [[CrossRef](#)]
29. Marsz, A.A.; Styszyńska, A. Intensity of thermohaline circulation in the North Atlantic and droughts in Poland. *Pr. I Stud. Geogr.* **2021**, *66*, 63–80. (In Polish) [[CrossRef](#)]
30. Knight, J.R.; Allan, R.J.; Folland, C.K.; Vellinga, M.; Mann, M.E. A signature of persistent natural thermohaline circulation cycles in observed climate. *Geophys. Res. Lett.* **2005**, *32*, L20708. [[CrossRef](#)]
31. Semenov, V.A.; Latif, M.; Dommenges, D.; Keenlyside, N.S.; Strehtz, A.; Martin, T.; Park, W. The impact of North Atlantic—Arctic Multidecadal Variability on Northern Hemisphere Surface Air Temperature. *J. Clim.* **2010**, *23*, 5668–5677. [[CrossRef](#)]
32. Farat, R.; Kepińska-Kasprzak, M.; Magier, P. Droughts in Poland in 1951–1990. In *Materiały Badawcze IMGW; Gospodarka Wodna i Ochrona Wód*: Warsaw, Poland, 1995; Volume 16, pp. 1–140. (In Polish)
33. Szyga-Pluta, K. Variability of the occurrence of droughts during the growing season in Poland in the years 1966–2015. *Przegląd Geofiz.* **2018**, *63*, 51–67. (In Polish)
34. Ilnicki, P.; Farat, R.; Górecki, K.; Lewandowski, P. Impact of climatic change on river discharge in the driest region of Poland. *Hydrol. Sci. J.* **2014**, *59*, 1117–1134. [[CrossRef](#)]
35. Peel, M.C.; Finlayson, B.L.; McMahon, T.A. Updated world map of the Köppen-Geiger climate classification. *Hydrol. Earth Syst. Sci.* **2007**, *11*, 1633–1644. [[CrossRef](#)]
36. Woś, A. *Climate of Poland in the Second Half of the 20th Century*; Wydawnictwo Naukowe UAM: Poznań, Poland, 2010. (In Polish)

37. Paślawski, Z.; Koczorowska, J.; Olejnik, K. Average Runoff in the Warta River Catchment. *Gospod. Wodna* **1972**, *6*, 214–218. (In Polish)
38. Perz, A.; Sobkowiak, L.; Wrzesiński, D. Spatial Differentiation of the Maximum River Runoff Synchronicity in the Warta River Catchment, Poland. *Water* **2020**, *12*, 1782. [[CrossRef](#)]
39. Dynowska, I. Regime of River Flow Sheet: 32.3. In *Atlas of the Republic of Poland*; IG PZ PAN: Warsaw, Poland, 1994. (In Polish)
40. Rotnicka, J. Typology of Hydrological Periods for Use in River Regime Studies. *Quaest. Geogr.* **1993**, *15/16*, 77–95.
41. Kalnay, E.; Kanamsitu, M.; Kistler, R.; Collins, W.; Deaven, D.; Gandin, L.; Iredell, M.; Saha, S.; White, G.; Woollen, J.; et al. The NCEP/NCAR 40-Year Reanalysis Project. *Bull. Am. Meteorol. Soc.* **1996**, *77*, 437–472. [[CrossRef](#)]
42. Vangengeim, G.Y. *Fundamentals of Macrocirculation Method for Long-Range Weather Forecasting for the Arctic*; Trudy AANII: Moscow, Russia, 1952; pp. 1–34. (In Russian)
43. Girs, A.A. On the creation of a single classification of the Northern Hemisphere. *Meteorol. I Gidrol.* **1964**, *4*, 43–47. (In Russian)
44. Dimitriev, A.A.; Dubravin, V.F.; Belyazo, V.A. *Atmospheric Processes of the Northern Hemisphere (1891–2018) and Their Use*; Super Izdatelstvo: Sankt-Petersburg, Russia, 2018. (In Russian)
45. Huang, B.; Thome, P.W.; Banzon, V.F.; Boyer, T.; Cherupin, G.; Lawrimore, J.H.; Menne, M.J.; Smith, T.M.; Vose, R.S.; Zhang, H.-M. Extended Reconstructed Sea Surface Temperature, version 5 (ERSSTv5): Upgrades, validation and intercomparisons. *J. Clim.* **2017**, *30*, 8179–8205. [[CrossRef](#)]
46. Tokarczyk, T. Drought assessment indicators used in Poland and in the world. *Infrastrukt. I Ekol. Teren. Wiej.* **2008**, *7*, 167–182. (In Polish)
47. Hill, T.; Lewicki, P. *Statistics: Methods and Applications*; StatSoft: Tulsa, OK, USA, 2007.
48. StatSoft, Inc. *Electronic Statistics Textbook*; Electronic Version; StatSoft: Tulsa, OK, USA, 1981–2011.
49. de Martonne, E. L'indice d'aridité. *Bull. De L'association De Géographes Français* **1926**, *9*, 3–5. (In French) [[CrossRef](#)]
50. Okołowicz, W. *General Climatology*; PWN—Polish Scientific Publishers: Warsaw, Poland, 1976.
51. Fortak, H. *Meteorology*; Deutsche Buch-Gemeinschaft: Berlin, Germany, 1971; pp. 1–287. (In German)
52. Harman, J.R.; Oliver, J.E. Rossby Wave/Rossby Number. In *Encyclopedia of World Climatology*; Encyclopedia of Earth Sciences Series; Oliver, J.E., Ed.; Springer: Dordrecht, The Netherlands, 2005. [[CrossRef](#)]
53. Marsz, A.A. Frequency of macro-types of mid-tropospheric circulation according to the Vangengeim-Girs classification in winter and the atmospheric pressure field over Europe and Northern Asia. *Przegląd Geofiz.* **2013**, *58*, 3–24. (In Polish)
54. Degirmendžić, J.; Kożuchowski, K. Macro-circulation as a conditioning factor for long-lasting thermal waves in Poland. *Przegląd Geofiz.* **2017**, *62*, 3–28. (In Polish)
55. Marsz, A.A.; Sobkowiak, L.; Styszyńska, A.; Wrzesiński, D. Causes and course of climate change and its hydrological consequences in the Greater Poland region in 1951–2020. *Quaest. Geogr.* **2022**, *41*, 183–206. [[CrossRef](#)]
56. Wrzesiński, D.; Marsz, A.A.; Sobkowiak, L.; Styszyńska, A. Response of Low Flows of Polish Rivers to Climate Change in 1987–1989. *Water* **2022**, *14*, 2780. [[CrossRef](#)]
57. Degirmendžić, J.; Kożuchowski, K. Variability of mid-tropospheric circulation forms according to Vangengeim-Girs classification and their relations to sea-level pressure patterns. *Przegląd Geofiz.* **2018**, *63*, 89–122. (In Polish)
58. Degirmendžić, J.; Kożuchowski, K. Variation of macro-circulation forms over the Atlantic-Eurasian temperate zone according to the Vangengeim-Girs classification. *Int. J. Climatol.* **2019**, *39*, 4938–4952. [[CrossRef](#)]
59. Savichev, A.I.; Mironicheva, N.P.; Cepelev, V.Y. Characteristics of atmospheric circulation fluctuations in the Atlantic-European sector of the hemisphere in recent decades. *Uchenye Zap. Ross. Gos. Gidrometeorol. Univ.* **2015**, *39*, 120–131. (In Russian)

Disclaimer/Publisher's Note: The statements, opinions and data contained in all publications are solely those of the individual author(s) and contributor(s) and not of MDPI and/or the editor(s). MDPI and/or the editor(s) disclaim responsibility for any injury to people or property resulting from any ideas, methods, instructions or products referred to in the content.